Direct measurement of groundwater flux in aquifers within the discontinuous permafrost zone: an application of the finite volume point dilution method near Umiujaq (Nunavik, Canada)

Journal:	*Hydrogeology Journal*
Manuscript ID	HJ-2018-5483.R2
Category:	Paper
Date Submitted by the Author:	n/a
Complete List of Authors:	Jamin, Pierre; University of Liège, Urban and Environmental Engineering Cochand, Marion; Université Laval, Département de géologie et de génie géologique; Université Laval, Département de géologie et de génie géologique Dagenais, Sophie; Université Laval, Département de géologie et de génie géologique Lemieux, Jean-Michel; Universite Laval, Department of Geology and Geological Engineering Fortier, Richard; Université Laval, Département de géologie et de génie géologique; Center for Northern Studies, Université Laval Molson, John; Université Laval, Département de géologie et de génie géologique Brouyère, Serge; University of Liège, Urban & Environmental Engineering Research Unit
Keywords:	Finite Volume Point Dilution Method, Permafrost, Tracer test, groundwater flow, Canada

Direct measurement of groundwater flux in aquifers within the discontinuous permafrost zone: an application of the finite volume point dilution method near Umiujaq (Nunavik, Canada)

P. Jamin[1], M. Cochand[2,3], S. Dagenais[2,3], J.-M. Lemieux[2,3*], R. Fortier[2,3], J. Molson[2,3] and S. Brouyère[1]

[1] Liège Université, Département Urban and Environmental Engineering, Hydrogeology and Environmental Geology, Building B52, 4000 Sart Tilman, Belgium.

[2] Département de géologie et de génie géologique, 1065 avenue de la Médecine, Université Laval, Quebec (Quebec), Canada, G1V 0A6.

[3] Centre d'études nordiques, Université Laval, Quebec (Quebec), Canada, G1V 0A6.

Keywords

Finite Volume Point Dilution Method, Tracer test, Groundwater flow, Permafrost, Canada

NOTE TO COPYEDITOR – PLEASE INSERT THE FOLLOWING AS A FIRST-PAGE FOOTNOTE:

This article is part of the topical collection "Hydrogeology of a cold-region watershed near Umiujaq (Nunavik, Canada)"

Abstract

Permafrost thaw is a complex process resulting from interactions between the atmosphere, soil, water and vegetation. Although advective heat transport by groundwater at depth likely plays a significant role in permafrost dynamics at many sites, there is lack of direct measurements of groundwater flow patterns and fluxes in such cold-region environments. Here, the finite volume point dilution method (FVPDM) is used to measure in-situ groundwater fluxes in two sandy aquifers in the discontinuous permafrost zone, within a small watershed near Umiujaq, Nunavik (Quebec), Canada. The FVPDM theory is first reviewed, then results from four FVPDM tests are presented: one test in a shallow supra-permafrost aquifer, and three in a deeper sub-permafrost aquifer. Apparent Darcy fluxes derived from the FVPDM tests varied from 0.5×10^{-5} to 1.0×10^{-5} m/s, implying that advective heat transport from groundwater flow could be contributing to rapid permafrost thaw at this site. In providing estimates of the Darcy fluxes at the local scale of the well screens, the approach offers more accurate and direct measurements over indirect estimates using Darcy's law. The tests show that this method can be successfully used in remote areas and with limited resources. Recommendations for optimizing the test protocol are proposed.

1. Introduction

Permafrost in the northern hemisphere covers an area of approximately 23×10^6 km², which represents more than two times the area of countries like Canada or United States, and is likely to decrease by 30 to 75 % over the next century due to climate change (Grosse et al. 2011; Slater and Lawrence 2013). Onshore and offshore effects of permafrost degradation have already been observed in Alaska (USA), northern Canada, Sweden, Siberia and Tibet since the early 1990s (Romanovsky et al. 2010). Although increasing atmospheric temperatures is the known cause, permafrost thaw is difficult to predict since it is a very complex process resulting from the non-linear interaction between the atmosphere and ground surface including soils, snow cover, vegetation, surface water and groundwater.

Prior to about 2010, only heat conduction had been taken into account in most of the numerical models used for simulating permafrost dynamics and to forecast permafrost degradation. Numerous authors have shown, however, that groundwater flow and heat transport by advection through subsurface flow systems should be considered in order to better understand and predict permafrost dynamics (e.g. Wright et al. 2009; Rowland et al. 2011; de Granpré et al. 2012; McKenzie and Voss 2013; Frampton and Destouni 2015; Kurylyk et al. 2016).

Validation of these models is fundamental since the accuracy of their predictions can be compromised by non-linear coupling and feedback loops. For instance, since thermal conductivity increases with soil water content, groundwater flow through an initially unsaturated porous medium will promote heat transport and permafrost thaw. Thawing permafrost also releases water, which in turn promotes heat transport, creating a positive feedback loop (Wright et al. 2009). Permafrost thaw also increases the hydraulic conductivity and effective porosity of the soil, allowing groundwater flow and groundwater recharge through an active flow layer (Briggs et al. 2014). Although this effect was shown in numerous field and numerical studies (Walvoord and Strieg, 2007; St Jacques and Sauchyn 2009; Lyon and Destouni 2010; Ge et al. 2011; O'Donnell et al. 2012), the consequences of this enhanced recharge and groundwater flow on permafrost thaw itself have rarely been examined. The heat carried by groundwater advection is thus likely to increase the rate of permafrost thaw leading to additional feedback processes.

Although groundwater flow and advective heat transport has been found to be important for understanding permafrost dynamics, there is a lack of groundwater tracer data and direct measurements of groundwater parameters such as hydraulic head and hydraulic conductivity for determining flow patterns and groundwater fluxes in permafrost environments (Bense et al. 2012). The challenge to find suitable permafrost sites which are suitably instrumented with groundwater monitoring wells, difficulties in accessing these sites, as well as high costs for field work in northern regions are the main factors which limit the availability of field observations. Existing monitoring wells are often insufficient to allow the assessment of representative hydraulic gradients and realistic groundwater flow rates (Ireson et al. 2013).

In most hydrogeological studies, groundwater (Darcy) fluxes are usually calculated indirectly using Darcy's law which requires access to a network of groundwater monitoring wells sufficiently dense to provide acceptable measurements of the hydraulic gradient and hydraulic conductivity, the latter usually obtained from a pumping test or slug test. Although quite simple, this approach only provides a mean Darcy flux (on the scale of the well spacing) and can yield fluxes with significant margins of error due to uncertainties in the hydraulic gradient and hydraulic conductivity (Bright et al. 2002; Devlin and McElwee 2007).

A crucial need thus exists for more reliable and direct methods to measure groundwater fluxes in the north, and using single-well techniques where possible. Available single-well techniques include both passive and direct measurements. For example, passive methods for measuring groundwater flux include passive flux meters (PFMs, ex. Hatfield et al. 2004) and the iFLUX sampler (iFLUX, 2018). However, passive cartridges applied with these methods have only been developed for 2 and 4 inch

(50 and 101 mm) wells and could not be easily adapted for this specific field site which uses 1.5 inch (38 mm) wells.

Direct measurement methods such as the colloidal borescope (Kearl 1997), acoustic Doppler flowmeter (Wilson et al. 2001) and In-Well PVP (Osorno et al. 2018) have discrete vertical sampling points that allow measuring local flow velocities which can be significantly different than the average water flux along the entire length of the well-screen. Furthermore, the three cited systems have respective diameters of 1.7, 3 and 2 inches (43, 76 and 50 mm), which prevent their use in 1.5 inch (38 mm) wells. Among the other available methods of direct measurement of groundwater fluxes, the Finite Volume Point Dilution Method (FVPDM; Brouyère et al. 2008) is a promising candidate since it is not limited by the diameter of the piezometer and it has been successfully applied in a variety of geological settings (Goderniaux et al. 2010; Jamin et al. 2015).

In Nunavik (Quebec, Canada), which lies north of the 55° parallel within the province of Quebec, permafrost thaw and groundwater availability are critical issues (Fortier et al. 2011; Lemieux et al. 2016). Buteau et al. (2010) studied a typical permafrost mound located in a small watershed near the Inuit community of Umiujaq in Nunavik using a heat conduction model. However, they were only able to reproduce observed temperatures within the permafrost by applying an unreasonable geothermal heat flux twice the value expected in this study area.

Recent investigations at the Umiujaq site (Lemieux et al. 2016; Fortier et al. this issue*;* Lemieux et al. this issue) have shown that an aquifer is located below the permafrost mounds in the lower part of the watershed, in which groundwater flow could be inducing significant advective heat transport and thus could be contributing to permafrost thaw. To help better understand the controlling parameters on permafrost dynamics in this type of periglacial environment, numerical models of groundwater flow and advective-conductive heat transport, accounting for freezing and thawing, have been developed (Dagenais et al. 2017; Dagenais et al. this issue; Parhizkar et al. 2017). A critical component of these models is the groundwater flow rate (Darcy flux) in the aquifer below the permafrost mounds. Indeed, supported by long-term records of temperature within one of these permafrost mounds, the modelling results suggest that advective heat transport is an important mechanism driving permafrost dynamics (Dagenais et al. 2017; Dagenais et al. this issue).

Since this studied watershed only hosts a few piezometers which are not ideal for determining representative hydraulic gradients, a direct method for determining groundwater fluxes was needed. The aims of this study were therefore: (1) to provide a direct measurement of the in-situ groundwater Darcy flux using the Finite Volume Point Dilution Method (FVPDM) in four piezometers within the studied watershed in the discontinuous permafrost zone of Nunavik (Quebec), Canada, and (2) to evaluate the application of the FVPDM in harsh conditions with limited accessibility and on-site resources. To the authors' knowledge, this is the first application of this technique in a northern environment, in particular within a sub-permafrost aquifer. Moreover, the measured groundwater fluxes within the sub-permafrost aquifer in this watershed are used to constrain numerical modelling of advective-conductive heat transfer and to assess the impacts of groundwater flow on permafrost dynamics (Dagenais et al. this issue).

After a brief description of the environmental context, the experimental setup adopted for the FVPDM experiments is detailed. The results are then presented and discussed. Finally, a series of recommendations are formulated for the optimization of FVPDM measurements in remote environments.

2. Study area

Located along the eastern shore of Hudson Bay, the Inuit community of Umiujaq lies within the discontinuous permafrost zone in Nunavik (Quebec) (Fig. 1). The study site is within a 2 km² watershed located in the Tasiapik Valley, between the village of Umiujaq and the northern end of Lake Tasiujaq, into which it drains. Within this valley, two aquifers, one surficial and one deep, lie above the bedrock (Fortier et al. this issue; Fig. 2 and 3).

The thin and unconfined surficial aquifer is found in a Quaternary unit of littoral and intertidal sands which overlies a unit of silty marine sediments deposited during the postglacial marine transgression of the Tyrell Sea. The thickness of the surficial sand unit is greatest in the upper part of the valley where it can be 10 m thick, but this unit is very thin in the lower part of the valley. The silty marine sediments vary in thickness from 10 m in the central part of the valley up to 20 m in the eastern downgradient part of the valley. Being frost-susceptible, the freezing of silty sediments under cold-climate conditions forms ice-rich permafrost mounds which are scattered across the valley (Fig. 2 and 3). These raised periglacial landforms due to the localized frost heaving have an approximate diameter of a few tens of meters and a maximum thickness of around 25 m.

The deep aquifer is found in the coarse-grained fluvioglacial/moraine sediments unit overlying the bedrock (Fortier et al. this issue). While unsaturated in the upper part of the valley, this unit becomes saturated in the lower part of the valley. This aquifer is also unconfined in the upper part of the valley, and becomes confined below the layer of frozen silts in the lowermost part of the valley, where artesian conditions may occur in late fall and early winter. The hydraulic conductivity of this aquifer is relatively high and can reach 1 m/d (1.2×10^{-5} m/s) (Lemieux et al. 2016).

The Tasiapik Valley hosts the Immatsiak sub-network which is part of the provincial network of groundwater monitoring wells commissioned by the Government of Quebec to assess the impacts of climate change on groundwater resources (Government of Quebec 2018). The Immatsiak sub-network is composed of several shallow and deep piezometers installed at seven monitoring sites during the summer of 2012 (Fig. 2). The piezometers are oriented along a transect parallel to the axis of the valley from north-west to south-east (Fig. 2 and 3).

2.1 Piezometer details

Direct groundwater flux measurements were performed in four piezometers in the Tasiapik Valley watershed: three in the deep aquifer (piezometers Pz4, Pz6, and Pz9), and one in the shallow aquifer (piezometer Pz2) (Fig. 2 and 3). All piezometers are made of PVC tubing with inside diameters of 1.5 inches (38 mm) (Table 1). The deep aquifer piezometers were installed by first drilling down to the contact between the glacial deposits and bedrock, then drilling continued from 2 to 3 m into the bedrock to confirm the bedrock contact. The piezometer screen was then installed from the bottom of the drill hole in the bedrock up to a height of 5 m which implies that only about half of the piezometer screen was in contact with the fluvioglacial sediments aquifer. Two tested piezometers in the deep aquifer, Pz4 and Pz6, are located in the lower part of the valley while piezometer Pz9 is located in the steepest part of the valley where higher groundwater fluxes are expected (Fig. 3). The deep aquifer piezometers Pz4, Pz6, and Pz9 were drilled to depths of 33.3, 35.4 and 38.3 m, respectively (Fig. 3; Table 1). For these three piezometers, the depth to the water table relative to ground surface at the moment of the direct groundwater flux measurements in summer 2016 was 3.4, 12.7, and 31.78 m, respectively (Fig. 3; Table 1). Finally, one measurement was carried out in the piezometer Pz2 which is located in the shallow aquifer in the upper part of the valley (Fig. 2 and 3). The depth of this piezometer is 4.65 m and the water table was 2.95 m below ground surface during the experiments (Table 1). This last piezometer was selected because advective heat transport within perched aquifers or shallow flow zones can also have an important effect on the dynamics of the underlying permafrost (Dagenais et al. this issue; Evans and Ge 2017; Frampton et al. 2013; Jiang et al. 2012).

3. Methodology

3.1 Theory of the FVPDM for flux measurements

For the experiments using the single-well point dilution method (PDM), the concentration evolution of an injected tracer is related to the intensity of the groundwater Darcy flux. The standard PDM involves a single instantaneous injection of tracer in the tested well and monitoring the decrease in tracer concentration over time due to dilution by groundwater flowing through the well screen. During the experiment, the water column inside the well is mixed to ensure a homogeneous distribution of the tracer mass. The Finite Volume Point Dilution Method (FVPDM) (Brouyère et al. 2008) is a generalization of the PDM where a continuous injection of the tracer into the well is used instead of only a single instantaneous injection of tracer. The FVPDM provides very good accuracy for measurements of steady state groundwater flow (Jamin et al. 2015).

The typical evolution of tracer concentrations in a well being tested using the FVPDM can be summarized as follows (Jamin and Brouyère 2018). At the beginning of the test, when the tracer injection starts, the tracer concentration within the tested well increases until the groundwater and tracer mass fluxes reach equilibrium. This first phase is the initiation phase in which the duration depends mainly on the groundwater flow rate passing through the well screen and on the mixing volume. The time to reach this stabilization is longer for larger mixing volumes and slower groundwater velocities.

A FVPDM test can be directly interpreted using the following analytical solution (Brouyère et al. 2008):

$$C_w(t) = \frac{Q_{inj}\,C_{inj} - \left(Q_{inj}\,C_{inj} - \left(Q_{inj} + Q_t\right)C_{w,0}\right)e^{-\frac{Q_{inj} + Q_t}{V_w}(t - t_0)}}{Q_{inj} + Q_t} \qquad (1)$$

where $C_w(t)$ [ML^{-3}] is the tracer concentration in the well at time t [T], C_{inj} [ML^{-3}] is the tracer concentration in the injected tracer fluid, $C_{w,0}$ [ML^{-3}] is the tracer concentration in the well at initial time t_0 [T], Q_{inj} [L^3T^{-1}] is the tracer fluid injection flow rate, V_w[L^3] is the volume of water in the injection well, and Q_t [L^3T^{-1}] is the (transit) flow rate of groundwater through the well screen during the FVPDM test.

If the groundwater velocity in the aquifer does not vary with time, and the tracer injection is long enough, the tracer concentration in the tested well will stabilize at a given value $C_{w,stab}$ proportional to the steady-state Darcy flux. This concentration plateau ensures good accuracy of the groundwater flux measurement because at this moment of the experiment, the tracer concentration in the well only depends on the groundwater flux and no longer depends on the mixing volume (see equation 16 in Brouyère et al. 2008).

The groundwater flux measured by the FVPDM is a direct in-situ measurement of the groundwater flux at the well screen. The accuracy of the results only depends on the quality of the field equipment, and particularly on the accuracy and stability of the tracer injection flow rate and measurements of tracer concentration in the well. The classical PDM measurements are also presented herein since the PDM-derived groundwater fluxes were used as an estimate of the first local groundwater flux allowing an optimal design of the full FVPDM experiment. The PDM is less accurate than the FVPDM because the PDM also depends on the accuracy of the estimated mixing volume (V_w) (see Brouyère et al. 2008 and Jamin et al. 2015 for more details), but the PDM test takes much less time to perform. Since the classical PDM can be considered as a specific case of the FVPDM where no tracer is injected during the monitoring phase of the test, the relationship between observed concentration in the well and groundwater flux during a PDM can be obtained from Eq. 1 by specifying Q_{inj} = 0, thus:

$$C_w(t) = C_{w,0} \times e^{-\frac{Q_t}{V_w}(t - t_0)} \quad (2)$$

The transit flow rate (Q_t) is calculated from a plot of ln ($C_w(t)$ / $C_{w,0}$) as a function of time, where the slope of this relationship is Q_t / V_w (Drost et al. 1968). The geometry of the well and circulation loop allows to estimate the mixing volume V_w and to calculate Q_t.

This last parameter Q_t is directly related to an apparent Darcy flux q_D [LT^{-1}] by the cross-sectional area S_w [L^2] perpendicular to groundwater flow (Equation 3). This cross–sectional area can be easily calculated by multiplying the well screen length (e_{scr}) [L] by the diameter of the well (2 r_w) [L], provided that the entire screen lies within a homogeneous porous medium. As for all other single well groundwater flux measurements, the apparent Darcy flux q_{app} [LT^{-1}], is related to the effective Darcy flux in the aquifer q_D by a flow distortion coefficient α_w that accounts for the convergence or divergence of the flow field in the vicinity of the borehole (Drost et al. 1968). Thus the apparent Darcy flux q_{app} is given by:

$$q_{app} = \alpha_w \, q_D = \frac{Q_t}{S_w} = \frac{Q_t}{2 \, r_w \, e_{scr}} \quad (3)$$

The flow field distortion coefficient α_w can be calculated on the basis of geometrical properties of the piezometer tubing and borehole, and on the hydraulic conductivities of the aquifer, of the filter pack and of the piezometer screen (Drost et al. 1968; Klammler et al. 2007; Verreydt et al. 2015). For the piezometers used in this study, only limited information was available on the hydraulic conductivity of the piezometer screen and of the sand filter pack. Consequently, the authors did not attempt to calculate what would be a dubious estimate of α_w. At best, and with reasonable assumptions, α_w can be considered to be in the range of 1.8 to 2.4. Hereafter, the term Darcy flux will refer implicitly to the apparent Darcy flux.

3.2 Experimental setup

The general setup for a FVPDM experiment consists of two pumps and one detector (Fig. 4). One pump, which can be a submersible pump or a surface pump depending on the depth to the water table, is used to mix the water column in the well, while the second pump is used to inject the tracer fluid into the well at a controlled low flow rate. Good accuracy and precision on the tracer injection flow rate is important since it controls the accuracy of the groundwater flux estimate. A detector is used to quantify the tracer concentration, preferably installed in the well or at the surface, and in-line with the circulation loop to monitor the evolution of tracer concentration over time.

Three types of pumps were tested in the piezometers of the studied watershed to mix the water column: a submersible pump (Supernova 36 SDEC France), a peristaltic pump (Waston Marlow 520 SN-REL) and a bladder pump (Solinst 407 Integra 1''). The circulation loops were made of either 10/13 mm or 4/6 mm nylon tubing. At the surface, a GGUN FL30 fluorometer was connected in line with the circulation loop to monitor the evolution of tracer concentrations (C_w) in the tested piezometer. An electromagnetic dosing pump (Magdos LT, Lutz-Jesco, GmbH) was connected to the loop to inject a fluorescent dye tracer (Uranine CAS n° 518-47-8). Finally, the circulation loop was returned down into the piezometer as far as the top of the groundwater level for experiments carried out on Pz2 and Pz9, or at the top of the water column when limited by a packer at Pz4 and Pz6. Groundwater levels were manually monitored during each experiment. Details of the experimental setup applied for each experiment are given in Table 1.

3.3 Interpretation of dilution tests

The results of the PDM experiments were interpreted using the exponential decrease of the tracer concentration (Equation 2); the calculation of a linear regression of the logarithm of the tracer concentration data as a function of time provided the slope of the relationship between these variables equal to the ratio Q_t / V_w. The corresponding apparent Darcy flux was then calculated using Equation 3.

The effective length of the piezometer screen (e_{scr}) used to determine the cross-sectional flow area (S_w) is defined as the portion of the screen exposed within the glacial deposits. The part of the screen in contact with the bedrock underlying the glacial deposits was assumed to have no influence on groundwater flow through the test well.

For the FVPDM test, the groundwater fluxes were calculated by using a least square optimization to fit the analytical solution (Equation 1) to the experimental data. The accuracy of the fit of the analytical solution to the experimental data was evaluated by a Bayesian approach proposed by Jamin et al. (2015). A set of 500 groundwater flux values (q_D) and mixing volumes (V_w) are first defined between realistic minimum and maximum limits. Each pair of q_D and V_w values was then used in Equation 1 with the corresponding parameters of the experimental setup to model the evolution of tracer concentration versus time. The sum of the residuals between the model and the observations was used to compute a probability density function. From each probability density function, the uncertainty of the fit of the Darcy flux was then defined by the confidence intervals of 5 and 95%.

3.4 Operational challenges

The FVPDM experiment offers a direct measurement of groundwater flux, independent of any measurement of aquifer parameters such as hydraulic conductivity or water levels. Nevertheless, the design of an FVPDM experiment requires an *a priori* estimate of the groundwater flux to optimize the tracer injection flow rate and injected tracer concentration (Brouyère et al. 2008). For the experiments in the piezometers of the Tasiapik Valley watershed, the first challenge was that the Darcy flux estimates in the aquifer were highly uncertain because of the limited number of piezometers where measurements of hydraulic conductivity had been performed, and because of the irregular spatial distribution of piezometric head measurements. The results of the *a priori* estimate of the Darcy flux in the vicinity of the tested piezometers, based on hydraulic gradients and hydraulic conductivity measured with slug tests (Fortier et al. 2014), are given in Table 2. At piezometer Pz2 in the shallow aquifer, the mean Darcy flux was estimated to be about 0.07 m/d using groundwater levels measured in four nearby piezometers in July 2014, 2015 and 2016. For piezometers Pz4 and Pz9 in the deeper aquifer, the estimated mean Darcy fluxes were 0.008 and 0.017 m/d, respectively. At piezometer Pz6 (also in the deeper aquifer), the estimated Darcy flux is one order of magnitude higher (0.49 m/d) compared to the other piezometers located in the same fluvioglacial aquifer. However, the difference could be due to an over-estimation of the hydraulic conductivity following the slug tests performed in 2014 (Fortier et al. 2014).

As detailed in Brouyère et al. (2008), increasing the tracer injection flow rate (Q_{inj}) close to the critical flow rate (Q_{cr}) decreases the time needed to reach the stabilized concentration plateau, insuring better accuracy of the experiment. A two-step procedure was thus used to conduct a FVPDM test with the optimal injection parameters, *i.e.* with an optimized tracer injection flow rate as close as possible to the critical injection flow rate (Q_{cr}) and injected tracer concentration. The first step consisted of a classical PDM test, which was designed using the estimated Darcy flux from the observed heads and hydraulic conductivity. For this first PDM, the mixing volume was calculated based on the geometry of the piezometer (diameter and height of the water column) and on the diameter and length of the circulation loop tubing. The PDM-based estimate of the groundwater flux around the tested piezometer was then used to optimize the full FVPDM test.

The second challenge was related to the geometry of piezometers Pz4, Pz6 and Pz9, which had short screen lengths (4.58 - 6.09 m) located at the bottom of deep boreholes (33.27 - 38.30 m deep). The shallow water levels in these piezometers implied that the water columns were very high relative to length of the screens. The mixing volume (V_w) was thus large, relative to the estimated groundwater flux across the small screens, leading to very long stabilization times for the FVPDM test. To illustrate the order of magnitude of the stabilization time, the dimensioning of a classical FVPDM test in piezometer Pz4 using the available data (V_w = 40 l, q_D = 0.008 m/d, S_w = 0.074 m²) led to estimated test durations of 90 days. Such a long test would have been impossible given the limited availability of a continuous power supply for the pumps, and the high cost of conducting a very long test in a remote area such as Umiujaq. In order to reduce the mixing volume, a custom-made double-flexible joint packer was built for isolating the screened section of the piezometers. This packer was installed in piezometer Pz4 at the top of the piezometer screen, reducing the mixing volume by 80 % and thus reducing the estimated stabilization time to less than 12 days. In piezometer Pz6, the packer reduced the mixing volume by 58 %. In piezometers Pz2 and Pz9, no packers were required for the FVPDM tests since the groundwater levels at these two piezometers were close to the top of the screen.

The last field-related challenges of performing FVPDM experiments at this test site were the difficult accessibility to the piezometers and the lack of a permanent power supply. Each FVPDM experiment had to run on a light portable electric generator for at least 24 hours. This limitation was overcome by using low electrical consumption pumps and by adaptation of an external fuel tank to the generator, increasing its autonomous operational range from 3 to 22 hours. The experiment could thus run autonomously and only needed manual filling of the fuel tank once or twice a day.

4. Results

The results of the point dilution experiment carried out in the four piezometers are presented in Figures 5 to 8, with the parameters of the PDM/FVPDM experimental setup provided in Table 1. For piezometers Pz2, Pz4, and Pz6, the results of the classical PDM test are first presented which are then followed by results from the FVPDM experiments. For piezometer Pz9, only a PDM experiment was performed due to the limited available time.

4.1 Piezometer Pz2

A classical point dilution experiment was first performed in piezometer Pz2 to quickly estimate the transit groundwater flow rate through the piezometer screen and to optimize the dimensions of the full FVPDM experiment. After a brief injection of Uranine, the tracer concentration was monitored in the tested piezometer for 5 hours (Fig. 5a). Considering a theoretical mixing volume of 7.9 l, calculated from the diameter and height of the water column and from the diameter and length of the circulation loop tubing, the estimated groundwater flow rate through the piezometer screen was 16.6 ml/min, which corresponds to a Darcy flux of 0.415 m/d.

The full FVPDM experiment was then performed over a period of 22 hours (Fig. 5b). Unfortunately, the pump used for mixing the water column in the piezometer overheated and failed 3 hours after the beginning of the tracer injection, preventing stabilization of the tracer concentration. The experimental setup was only repaired 12 hours later, which at least allowed monitoring the decrease in tracer concentrations. Notwithstanding these difficulties, the test results could be processed and interpreted, yielding an adjusted mixing volume of 9.41 l and an estimated Darcy flux of 0.776 ± 0.012 m/d.

4.2 Piezometer Pz4

A dilution experiment was performed in piezometer Pz4 over a period of 5.5 hours (Fig. 6a). Considering a theoretical mixing volume of 12.9 l, the estimated groundwater flow rate through the well screen was 36.7 ml/min, which corresponds to a Darcy flux of 0.720m/d. The mixing volume was limited by a packer installed at a depth of approximately 30.5 m.

The results of the full 30-hour FVPDM experiment, including a tracer injection period of 21 hours, are shown in Fig. 6b. No problems were encountered during this experiment. Based on the interpretation, a mixing volume of 8.51 l and a Darcy flux of 0.577 ± 0.006 m/d were derived for piezometer Pz4.

4.3 Piezometer Pz6

The dilution experiment in piezometer Pz6 lasted for 5.2 hours. Considering a theoretical mixing volume of 12.6 l, a volumetric groundwater flow rate of 57.7 ml/min was determined (Fig. 7a) which corresponds to a Darcy flux of 1.74 m/d. The mixing volume was limited by a packer installed approximately at 28.5 m deep.

The transit flow rate determined by the PDM test in this piezometer was slightly higher than in the other piezometers, allowing for a faster stabilization of the concentration during the FVPDM experiment. It was thus decided to apply two consecutive tracer injection flow rates for the FVPDM experimental setup in order to observe two stabilized tracer plateaus for a better accuracy on the interpreted Darcy flux (Fig. 6b). The full FVPDM experiment was conducted flawlessly over a period of 28 hours. The calculated Darcy flux in piezometer Pz6 is 0.733 ± 0.003 m/d and the adjusted mixing volume is 9.63 l.

4.4 Piezometer Pz9

Due to the piezometer setup, limited available time, and available pumps, only a PDM experiment was performed in the piezometer Pz9. Indeed, only a bladder pump and a peristaltic pump were available for this last experiment. After a brief injection of Uranine lasting for 20 minutes, the decrease in Uranine concentrations was monitored over a period of 3 hours (Fig. 8). The mixing volume was estimated at 7.56 l and the calculated Darcy flux in the piezometer Pz9 was 0.840 m/d. No uncertainty analysis was possible since only a PDM experiment was performed in this piezometer.

5. Discussion

Based on the FVPDM experiments performed in four piezometers in the Tasiapik Valley watershed, groundwater fluxes vary from 0.58 to 0.84 m/d which are significantly higher than initial estimates based on Darcy's law of 0.01 to 0.49 m/d using monitored water levels from previous years. It is also important to note that the Darcy fluxes measured by dilution tests in the piezometers are apparent Darcy fluxes which might overestimate the actual Darcy flux in the aquifer by a factor 1.8 to 2.4 according to the estimated flow field distortion coefficient. The Darcy flux for each tested piezometer was also estimated using groundwater levels measured at the time of the FVPDM experiments (Table 2). In piezometer Pz2, the Darcy flux calculated using Darcy's law and water levels from July 2017 is 11 times lower than the flux measured in the FVPDM experiment. In piezometers Pz4 and Pz9, the same estimates are respectively 72 and 48 times lower than the Darcy flux measured by the FVPDM experiments. On the other hand, the Darcy law-estimated groundwater flux in piezometer Pz6 is very close to the flux calculated from the FVPDM experiment. However, these results based on a simple application of Darcy's law are questionable due to the abnormally high value of hydraulic conductivity found at this location. These significant differences highlight the benefits of direct groundwater flux measurements. In this case, the number of available piezometers and their spatial distribution only provided a rough under-estimate of the hydraulic gradient for calculating fluxes based on Darcy's law. An explanation of this underestimation could be that the piezometers used to estimate the Darcy flux based on hydraulic gradients are not aligned along the main groundwater flow direction. Inaccurate hydraulic conductivity values determined from the slug tests could also explain the underestimation of the groundwater flux.

Groundwater fluxes within the deep aquifer decrease along the flow direction from piezometer Pz9 to Pz4, toward Lake Tasiujaq. This distribution of groundwater fluxes is consistent with the hydrogeological setting. The groundwater fluxes are higher near piezometer Pz9 where the deep aquifer is inclined with a steep water table, while they are lower near piezometer Pz4, where the water table is much flatter. In piezometer Pz6, the Darcy flux has an intermediate value of 0.733 m/d.

The Darcy flux in the unconfined perched aquifer in the upper part of the valley in piezometer Pz2 is relatively high (0.776 m/d) with regard to the overall topography of this upland area. This could be explained by the fact that this piezometer is located beside a permafrost mound that forms a local topographical high, about 2-3 m above the surrounding land elevation. Due to the dome shape of the mound, groundwater flows radially away from the mound which likely induces a higher than expected groundwater flux.

The maximum error in the calculated Darcy flux is about ±1 %. This high accuracy is due to the good experimental data, very low noise levels in the tracer concentration measurements and careful and frequent calibration of the fluorometer and tracer injection pumps. The duration of all FVPDM experiments was around 20 hours, which is relatively long for a single groundwater flux measurement. As mentioned in Jamin and Brouyère (2018), measuring groundwater fluxes lower than 0.1 m/d using the FVPDM technique may be challenging due to the long test duration required. However, in this study, a long-duration experiment allowed a long stabilized tracer concentration plateau, which significantly increased the accuracy of the results.

Several issues can be noted regarding the interpretation of the tests. First, the mixing volume adjusted by the interpretation of the FVPDM experiment is different from the theoretical mixing volume calculated based on the geometric properties of the well and of the circulation loop. For instance, for piezometer Pz2, the adjusted mixing volume is 20 % greater than the theoretical mixing volume. This difference could arise since some of the water present in the filter pack around the internal tubing of the piezometer is likely involved in the mixing volume. For piezometers Pz4 and Pz6, the adjusted mixing volume is 28 and 17 % less than the theoretical mixing volume. Packers were used in both of these piezometers for reducing the mixing volume. This volume might have been underestimated due to inaccuracy in the installation depth of the packers (1.1 l per meter depth error), and due to the volume of the submersible pump used to mix the water (approximately 0.4 l), which was not taken into account, and which would therefore reduce the current mixing volume.

Furthermore, at each tested piezometer, the Darcy fluxes determined from the PDM experiments differ from those determined from the FVPDM experiments. This difference in fluxes between the two methods is likely due to the difference in mixing volumes considered in both cases. The PDM results were interpreted using a geometrically based theoretical mixing volume, while the Darcy fluxes assessed from the FVPDM experiments are independent of the mixing volume estimation. If the PDM-based Darcy fluxes had been calculated using the actual mixing volume adjusted for the interpretation of the FVPDM experiments, the results would have been closer to the FVPDM-based Darcy fluxes. An accurate estimation of the mixing volume is therefore critical for the interpretation of a PDM experiment.

Even if the accuracy of the groundwater fluxes depends on the accuracy of the fluorescent dye tracer concentrations, the piezometer setup also induces some uncertainties. These uncertainties originate from the installation depths of piezometers Pz4, Pz6, and Pz9 which are screened about half in the bedrock and half in the moraine sediments, each characterized by different hydraulic properties. For the interpretation of the dilution experiments, it was assumed that groundwater is only flowing within the moraine sediments and the flow cross-section area (S_w) thus only corresponds to the length of the piezometer's screen in the moraine sediments. This hypothesis was supported by a visual inspection of the rock cores sampled during drilling, which revealed massive structure with only few fractures. However, groundwater flow might also occur within these fractures. Because the flow cross-section has a direct impact on the groundwater flux assessment, choosing a flow section twice the actual value would have reduced the calculated flux by one-half. Since all piezometers in the deep aquifer have about the same configuration, the relative differences between the fluxes would have remained the same, but the absolute value would have changed. For piezometer Pz2, this is not an issue since this piezometer is only screened in the sandy sediments.

The equipment failure during the FVPDM experiment performed in piezometer Pz2 provided new insights for carrying out further FVPDM experiments. As a long-duration measurement, the FVPDM experiment requires flawless operation of all equipment, including the power generator, mixing pump, injection pump and tracer detector. Another aspect to consider is the power supply which should be able to run autonomously and flawlessly during the entire experiment, and be able to withstand the energy consumption of the pumps. The third critical point of the setup is the choice of robust and reliable pumps, particularly in such harsh and remote environments. In this study, the only available pump for mixing the water column was a peristaltic sampling pump, which is not designed to run continuously for several hours. Finally, the setup in the field should be secured against any disturbance either due to weather conditions (e.g. wind, rain or freezing temperatures in the tracer injection tank), animals or vandalism. The experimental setup could also be improved by integrating the equipment (pumps, detectors, hoses and connections) into a single portable unit, easily handled during transport and field operations. Nevertheless, the dilution experiment in piezometer Pz9 showed that even with limited equipment and time, it is possible to perform a valuable and accurate direct measurement of groundwater flux.

It is acknowledged that groundwater fluxes measured with the PDM and FVPDM experiments are only representative for the specific period of measurement in the field, while the magnitude of these fluxes may change throughout the year, especially in this type of environment where the ground is frozen almost seven months per year. As an example, water level variations up to 12 m were observed in piezometer Pz6 over a single year (2012-2013, Lemieux et al. this issue). Such transient changes in the flow system could be followed by repeating the FVPDM experiments over the different seasons.

The groundwater fluxes obtained from the FVPDM tests are critical independent data for constraining groundwater flow and heat transport models, and for estimating general thermal balances at the Umiujaq site. They can be used, for example, to estimate the relative contribution of convective heat transfer in the confined aquifer to heat transfer by conduction alone. One measure of this contribution is the Peclet number, defined as $Pe = \Delta L \; q_D \; \vartheta / \kappa$, where ΔL is a characteristic length (m), q_D is the Darcy flux (m/s), ϑ is the porosity and κ is the thermal diffusivity (m^2/s). The Peclet number is a dimensionless ratio between the heat transport by convection and by conduction. Assuming ΔL corresponds to the depth of the confined aquifer below the permafrost (~20 m), a porosity of 0.35, a thermal diffusivity of 8×10^{-7} m^2/s (Dagenais et al, this issue), and using the observed mean Darcy flux of 3.3×10^{-6} m/s ($q_D = q_{app} / \alpha_w = 0.6 / 2.1 = 0.29$ m/d), the Peclet number is about $Pe = 29$, which indicates a heat convection-dominated system. The important role of convective heat transport on permafrost degradation was confirmed in the numerical model of Dagenais et al (this issue).

6. Conclusions

The use of the FVPDM has provided reliable estimates of groundwater fluxes in a shallow supra-permafrost aquifer and in a deep sub-permafrost aquifer beside and below permafrost mounds in the discontinuous permafrost zone in Nunavik (Quebec), Canada. Measured apparent groundwater fluxes range from 0.577 to 0.840 m/d with respective accuracies varying from ±0.003 to ±0.012 m/d, which are consistent with the hydrogeological settings. These data are important since no groundwater fluxes are currently available in this type of periglacial environment. Moreover, these data are essential for constraining numerical models of advective-conductive heat transfer to better understand permafrost dynamics (see Dagenais et al. this issue).

During the PDM and FVPDM experiments carried out in four piezometers within the Tasiapik Valley watershed at Umiujaq, several major challenges were encountered such as small screen/borehole length ratios, small borehole diameters and harsh conditions in a remote environment. Nevertheless, all challenges were overcome, proving the versatility of the method. A key component of the successful application of these point dilution methods was the use of borehole packers for isolating the piezometer screen, which significantly reduced the duration of the experiments. Based on the experience gained from these experiments, robust equipment should be used and commercially available groundwater sampling pumps should be avoided.

Although the point dilution methods used in this study were useful to assess groundwater flux, the direction of groundwater flow remains unknown. Groundwater flow direction is valuable information for study sites such as the Tasiapik Valley watershed at Umiujaq where only a few boreholes are available and which are not optimally configured for standard application of Darcy's law. Ongoing development of the point dilution method should resolve this issue in the near future.

Piezometer	Type of dilution	Tubing radius	Tubing depth	Bedrock depth	Screen length	Effective screen length*	Water level depth	Packer depth	Circulation loop length	Circulation loop radius	Theoretical mixing volume	Mixing pump	Mixing flow rate	Injection pump	Tracer injection flow rate	Injected tracer conc.	Flow surface area
		[m]	[m]	[m]	[m]	[m]	[m]	[m]	[m]	[m]	[l]		[l/min]		[ml/min]	[ppb]	[m²]
Pz2	PDM	0.019	4.57	n.r.	1.52	1.52	2.955	n.n.	80	0.005	0.008	Peristaltic	3.500	Electromagnetic	n.a.	188.0	0.058
	FVPDM	0.019	4.57	n.r.	1.52	1.52	2.955	n.n.	80	0.005	0.008	Peristaltic	3.500	Electromagnetic	47	1627.7	0.058
Pz4	PDM	0.019	35.36	32.72	4.58	1.94	3.400	29.59	80	0.005	0.012	Peristaltic	2.015	Electromagnetic	n.a.	1627.7	0.074
	FVPDM	0.019	35.36	32.72	4.58	1.94	3.400	29.59	80	0.005	0.012	Peristaltic	2.015	Electromagnetic	45	1736.7	0.074
Pz6	PDM	0.019	33.27	29.90	4.64	1.27	12.690	27.74	80	0.005	0.012	Submersible	5.400	Electromagnetic	n.a.	195.4	0.048
	FVPDM	0.019	33.27	29.90	4.64	1.27	12.690	27.74	80	0.005	0.012	Submersible	5.400	Electromagnetic	50 / 29.9	195.4	0.048
Pz9	PDM	0.019	38.30	34.09	6.09	1.88	31.785	n.n.	80	0.002	0.008	Bladder	0.258	Electromagnetic	n.a.	188.0	0.072

Table 1: Details of the experimental setup for the point dilution method (PDM) and finite volume point dilution method (FVPDM) experiments near Umiujaq.

n.r. = not reached. n.n. = not needed. n.a. = not applicable. *Effective screen length is the part of the piezometer screen within the fluvioglacial sediments aquifer.

Piezometer	Hyraulic conductivity calculated from slug tests	Estimated Darcy flux based on hydraulic gradient and hydraulic conductivity				Measurements based on PDM experiments			Measurements based on FVPDM experiments			
		2014	2015	2016	2017	Theoretical mixing volume	Estimated transit flow rate	Estimated Darcy flux	Adjusted mixing volume	Adjusted transit flow rate	Adjusted Darcy flux	Uncertainty on Darcy flux
	[m/d]	[m/d]	[m/d]	[m/d]	[m/d]	[l]	[l/min]	[m/d]	[l]	[l/min]	[m/d]	[m/d]
Pz2	4.25	0.066	0.075	0.070	0.070	7.90	0.017	0.415	9.41	0.031	0.776	±0.012
Pz4	0.85	0.007	0.008	0.009	0.008	11.88	0.037	0.716	8.51	0.030	0.577	±0.006
Pz6	13.82	0.500	0.487	0.486	0.506	11.68	0.058	1.719	9.63	0.025	0.733	±0.003
Pz9	0.27	0.018	0.017	0.016	0.017	7.56	0.042	0.840				

Table 2: Estimates of the groundwater flux based on Darcy's law using hydraulic conductivity and hydraulic gradient. Hydraulic conductivity was measured using slug tests (Fortier et al. 2014). Results of the PDM and FVPDM measurements show an apparent Darcy flux much higher than expected.

Acknowledgments

This work was supported by the University of Liège [grant no. FSRC-12/81], by the Belgian F.R.S.-FNRS research program [grant no. 1.5060.12], by the Fondation Roi Baudouin, Prix Ernst Dubois [grant no. 2015-F2812650-204355] and the Natural Sciences and Engineering Research Council of Canada (NSERC) through the Strategic Project Grant program. The authors wish to thank the Centre d'études nordiques (CEN) at Université Laval and the Inuit community of Umiujaq for supporting this research.

References

Commented [S1]: Yellow reference details will be corrected later

Allard M, Lemay M (2012) Nunavik and Nunatsiavut: from science to policy: an integrated regional impact study (IRIS) of climate change and modernization. ArcticNet, Quebec City, QC, 303 pp

Bense VF, Kooi H, Ferguson G, Read T (2012) Permafrost degradation as a control on hydrogeological regime shifts in a warming climate. *Journal of Geophysical Research: Earth Surface*, *117*(3), 1–18. doi:10.1029/2011JF002143

Briggs MA, Walvoord MA, McKenzie JM, Voss CI, Day-Lewis FD, Lane JW (2014) New permafrost is forming around shrinking Arctic lakes, but will it last? *Geophysical Research Letters*, *41*(5), 1585–1592. doi:10.1002/2014GL059251

Bright J, Wang F, Close M (2002) Influence of the amount of available K data on uncertainty about contaminant transport prediction. *Groundwater*. doi:10.1111/j.1745-6584.2002.tb02537.x

Brouyère S, Batlle-Aguilar J, Goderniaux P, Dassargues A (2008) A new tracer technique for monitoring groundwater fluxes: the Finite Volume Point Dilution Method. *Journal of Contaminant Hydrology*, *95*(3–4), 121–40. doi:10.1016/j.jconhyd.2007.09.001

Buteau S, Fortier R, Allard M (2010) Permafrost weakening as a potential impact of climatic warming. *Journal of Cold Regions Engineering*, *24*(1), 1–18. doi:10.1061/(ASCE)0887-381X(2010)24:1(1)

Dagenais S, Molson J, Lemieux J-M, Fortier R, Therrien R (2017) Coupled cryo-hydrogeological modelling of permafrost degradation at Umiujaq, Quebec, Canada. *GeoOttawa 2017, 12th Joint CGS/IAH-CNC Groundwater Conference, Ottawa, Canada, Oct. 1-4, 2017.*

Dagenais S, Molson J, Lemieux J-M, Fortier R, Therrien R (this issue) Coupled cryo-hydrogeological modelling of permafrost degradation at Umiujaq, Nunavik, Canada. *Hydrogeology Journal*.

de Grandpré I, Fortier D, Stephani E (2012) Degradation of permafrost beneath a road embankment enhanced by heat advected in groundwater. *Canadian Journal of Earth Sciences*, *49*(8), 953–962. doi:10.1139/e2012-018

Devlin JF, McElwee CD (2007) Effects of measurement error on horizontal hydraulic gradient estimates. *Groundwater*, *45*(1), 62–73. doi:10.1111/j.1745-6584.2006.00249.x

Drost W, Klotz D, Koch A, Moser H, Neumaier F, Rauert W (1968) Point dilution methods of investigating ground water flow by means of radioisotopes. *Water Resources Research*, 4(1), 125–146. Retrieved from http://www.agu.org/pubs/crossref/1968/WR004i001p00125.shtml

Evans SG, Ge S (2017) Contrasting hydrogeologic responses to warming in permafrost and seasonally frozen ground hillslopes. Geophys. Res. Lett., 44. doi:10.1002/2016GL072009

Fortier R, LeBlanc A-M, Yu W (2011) Impacts of permafrost degradation on a road embankment at Umiujaq in Nunavik (Quebec), Canada. *Canadian Geotechnical Journal*, *48*(5), 720–740. doi:10.1139/t10-101

Fortier R, Lemieux J-M, Molson J, Therrien R (2013) Rapport de la phase III du projet de déploiement du réseau Immatsiak: Campagne de forages pour l'installation de puits d'observation des eaux souterraines dans un petit bassin versant pergélisolé à Umiujaq (in French) [Phase III Report of the Immatsiak Network Deployment Project: Drilling Campaign for the Installation of Groundwater Wells in a Small Permafrost Watershed in Umiujaq]. Technical report. Université Laval, Centre d'Etudes Nordiques, 89p.

Fortier R, Lemieux J-M, Talbot-Poulin M-C, Banville D-R, Lévesque R, Molson J, Therrien R (2014) Rapport de la phase IIIb du déploiement du réseau Immatsiak: Hydrogéologie d'un bassin versant dans une vallée près d'Umiujaq (in French) [Immatsiak Network Phase IIIb Report: Hydrogeology of a Watershed in a Valley Near Umiujaq]. Technical report. Université Laval, Centre d'Etudes Nordiques, 275p.

Fortier R, Roy-Banville D, Lévesque R, Lemieux J-M, Molson J, Therrien R, Ouellet M (this issue) Development of a 3D cryohydrogeological model of a small watershed in a degrading permafrost environment in Umiujaq, Nunavik, Canada. *Hydrogeology Journal.*

Frampton A, Destouni G (2015) Impact of degrading permafrost on subsurface solute transport pathways and travel time. *Water Resources Research*, 1–22. doi:10.1002/2014WR016689

Frampton A, Painter SL, Destouni G (2013), Permafrost degradation and subsurface flow changes caused by surface warming trend., Hydrogeology Journal, 21(1), 271–280. doi: 10.1007/s10040-012-0938-z

Ge S, McKenzie J, Voss C, Wu Q (2011) Exchange of groundwater and surface-water mediated by permafrost response to seasonal and long term air temperature variation. *Geophysical Research Letters*, *38*(14), 1–6. doi:10.1029/2011GL047911

Goderniaux P, Brouyère S, Gutierrez A, Baran N (2010) Multi-tracer tests to evaluate the hydraulic setting of a complex aquifer system (Brévilles spring catchment, France) *Hydrogeology Journal*, *18*(7), 1729–1740. doi:10.1007/s10040-010-0633-x

Government of Quebec (2019) Réseau de suivi des eaux souterraines du Quebec. Retrieved from http://www.environnement.gouv.qc.ca/eau/piezo/index.htm Cited 2 February 2019.

Grosse G, Romanovsky V, Jorgenson T, Anthony KW, Brown J, Overduin PP (2011) Vulnerability and feedbacks of permafrost to climate change. EOS, Transactions, American Geophysical Union, 92(9), 73–80. doi:10.1029/2011EO090001

Hatfield K, Annable M, Cho J, Rao PSC, Klammler H (2004) A direct passive method for measuring water and contaminant fluxes in porous media. Journal of Contaminant Hydrology, 75 (3–4), 155-181. http://doi.org/10.1016/j.jconhyd.2004.06.005

iFLUX (2019) iFLUX sampling, envison groundwater in motion. Retrieved from http://www.ifluxsampling.com Cited 2 February 2019.

Ireson AM, van der Kamp G, Ferguson G, Nachshon U, Wheater HS (2013) Hydrogeological processes in seasonally frozen northern latitudes: understanding, gaps and challenges. *Hydrogeology Journal*, *21*(1), 53–66. doi:10.1007/s10040-012-0916-5

Jamin P, Goderniaux P, Bour O, Le Borgne T, Englert A, Longuevergne L, Brouyère S (2015) Contribution of the finite volume point dilution method for measurement of groundwater fluxes in a fractured aquifer. *Journal of Contaminant Hydrology*, 182, 244-255. https://doi.org/10.1016/j.jconhyd.2015.09.002

Jamin P, Brouyère S (2018) Monitoring transient groundwater fluxes using the Finite Volume Point Dilution Method. *Journal of Contaminant Hydrology, 218, 10-18*. https://doi.org/10.1016/j.jconhyd.2018.07.005

Jiang Y, Zhuang Q, O'Donnell JA (2012) Modeling thermal dynamics of active layer soils and near-surface permafrost using a fully coupled water and heat transport model, J. Geophys. Res., 117, D11110. doi:10.1029/2012JD017512

Kearl PM (1997) Observations of particle movement in a monitoring well using the colloidal borescope, Journal of Hydrology, 200, 1-4, 323-344. https://doi.org/10.1016/S0022-1694(97)00026-7

Klammler H, Hatfield K, Annable MD, Agyei E, Parker BL, Cherry JA, Rao PSC (2007) General analytical treatment of the flow field relevant to the interpretation of passive fluxmeter measurements, *Water Resources Reseach*, 43, W04407, doi:10.1029/2005WR004718

Kurylyk BL, Hayashi M, Quinton WL, McKenzie JM, Voss CI (2016), Influence of vertical and lateral heat transfer on permafrost thaw, peatland landscape transition, and groundwater flow, *Water Resources. Research*, 52, 1286–1305, doi:10.1002/ 2015WR018057

Kurylyk BL, MacQuarrie KTB, Voss CI (2014) Climate change impacts on the temperature and magnitude of groundwater discharge from shallow, unconfined aquifers. *Water Resources Research*, *50*(4), 3253–3274. doi:10.1002/2013WR014588

Lemieux J-M, Fortier R, Murray R, Dagenais S, Cochand M, Delottier H, Therrien R, Pryet A, Parhizkar M (this issue) Groundwater dynamics within a discontinuous permafrost watershed, Umiujaq, Nunavik, Canada. *Hydrogeology Journal*.

Lemieux JM, Fortier R, Talbot-Poulin MC, Molson J, Therrien R, Ouellet M, Banville D, Cochand M, Murray R (2016) Groundwater occurrence in cold environments: examples from Nunavik, Canada. *Hydrogeology Journal*, *24*(6), 1497–1513. doi:10.1007/s10040-016-1411-1

Lyon SW, Destouni G (2010) Changes in catchment-scale recession flow properties in response to permafrost thawing in the Yukon River Basin. *International Journal of Climatology*, *30*(14), 2138–2145. doi:10.1002/joc.1993

Martin D, Belanger D, Gosselin P, Brazeau J, Furgal C, Dery S (2007) Drinking water and potential threats to human health in Nunavik: Adaptation strategies under climate change conditions. *Arctic*, *60*(2), 195–202. doi:http://dx.doi.org/10.14430/arctic244

McKenzie JM, Voss CI (2013) Permafrost thaw in a nested groundwater-flow system. *Hydrogeology Journal*, *21*(1), 299–316. doi:10.1007/s10040-012-0942-3

O'Donnell JA, Aiken GR, Walvoord MA, Butler KD (2012) Dissolved organic matter composition of winter flow in the Yukon River basin: Implications of permafrost thaw and increased groundwater discharge. *Global Biogeochemical Cycles*, *26*(4), 1–18. doi:10.1029/2012GB004341

Osorno TC, Devlin JF, Firdous R (2018) An In-Well Point Velocity Probe for the rapid determination of groundwater velocity at the centimeter-scale, Journal of Hydrology, 557, 539-546. https://doi.org/10.1016/j.jhydrol.2017.12.033

Parhizkar M, Therrien R, Molson J, Lemieux J-M, Fortier R, Talbot-Poulin M-C, Therrien P, Ouellet M (2017) An integrated surface-subsurface flow model of the thermo-hydrological behavior and effect of climate change in a cold-region watershed in northern Quebec, Canada. *GeoOttawa 2017, 12th Joint CGS/IAH-CNC Groundwater Conference, Ottawa, Canada, Oct. 1-4, 2017*.

Romanovsky VE, Smith SL, Christiansen HH (2010) Permafrost thermal state in the polar northern hemisphere during the international polar year 2007-2009: A synthesis. Permafrost and Periglacial Processes, 21(2), 106–116. doi:10.1002/ppp.689

Rowland JC, Travis BJ, Wilson CJ (2011) The role of advective heat transport in talik development beneath lakes and ponds in discontinuous permafrost. *Geophysical Research Letters*, *38*(17), 1–5. doi:10.1029/2011GL048497

Slater AG, Lawrence DM (2013) Diagnosing present and future permafrost from climate models. Journal of Climate, 26(15), 5608–5623. doi:10.1175/JCLI-D-12-00341.1

St. Jacques JMS, Sauchyn DJ (2009) Increasing winter baseflow and mean annual streamflow from possible permafrost thawing in the Northwest Territories, Canada. *Geophysical Research Letters*, *36*(1), 1–6. doi:10.1029/2008GL035822

Verreydt G, Bronders J, Van Keer I, Diels L, Vanderauwera P (2015) Groundwater Flow Field Distortion by Monitoring Wells and Passive Flux Meters. Groundwater, 53, 933-942. doi:10.1111/gwat.12290

Walvoord MA, Striegl RG (2007) Increased groundwater to stream discharge from permafrost thawing in the Yukon River basin: Potential impacts on lateral export of carbon and nitrogen. *Geophysical Research Letters*, *34*(12) doi:10.1029/2007GL030216

Wright N, Hayashi M, Quinton WL (2009) Spatial and temporal variations in active layer thawing and their implication on runoff generation in peat-covered permafrost terrain. *Water Resources Research*, *45*(5), 1–13. doi:10.1029/2008WR006880

FIGURE CAPTIONS:

Fig. 1: Maps of Canada and permafrost extent and types in Nunavik (Quebec; Allard and Lemay 2012). The experiments were carried out near Umiujaq, an Inuit community located on the east coast of Hudson Bay, in the discontinuous permafrost zone, in Nunavik (Quebec), Canada. The studied 2 km² watershed is located near Umiujaq at the northern end of Lake Tasiujaq, into which it drains.

Fig. 2: Map of the Quaternary deposits in the Tasiapik Valley. Location of the piezometers and cross-section in the Tasiapik Valley. Projected coordinate system: NAD 1983 MTM Zone 9.

Fig. 3: Cross-section of Quaternary deposits in the Tasiapik Valley (see Figure 2 for location). The upper sediment layers are composed of littoral sands and marine silts invaded by permafrost. The uppermost sand layer contains an unconfined perched aquifer. A deep aquifer is found in the coarse-grained fluvioglacial sediments at depth overlying the bedrock. Among the four tested piezometers, three are located in the deep aquifer while one is in the surficial aquifer. Note: for piezometers Pz4, Pz6, and Pz9, only the part of each screen that is located in the deep aquifer is considered representative of the flow system for the calculation of groundwater fluxes. The Darcy fluxes measured within the piezometers installed in the fluvioglacial sediments decrease along the flow direction of the Tasiapik Valley toward Lake Tasiujaq.

Fig. 4: Experimental setup of the FVPDM. The water volume within the well is constantly mixed using a pump and circulated to the surface, where a tracer is injected using a dosing pump. Tracer concentration in the loop is monitored using a field fluorometer placed in-line. A packer was installed in piezometers Pz4 and Pz6 to limit the mixing volume, hence shortening the time required for the FVPDM experiment.

Fig. 5: Experimental results in piezometer Pz2 (see Figures 2 and 3 for location). (a) The first PDM dilution experiment provided a groundwater transit flow rate estimate of 15.2 ml/min passing through the piezometer screen. (b) The estimated groundwater flux is 0.78 m/d. A failure of the mixing pump prevented the measurement and stabilization of the tracer concentration during the FVPDM experiment. (C_w* = normalized Uranine tracer concentration C_w / C_{inj})

Fig. 6: Experimental results in piezometer Pz4 (see Figures 2 and 3 for location). (a) The first dilution experiment provided a groundwater transit flow rate estimate of 36.7 ml/min passing through the piezometer screen. (b) The measured groundwater flux is 0.58 m/d. (C_w* = normalized Uranine tracer concentration C_w / C_{inj})

Fig. 7: Experimental results in piezometer Pz6 (see Figures 2 and 3 for location). (a) The first dilution experiment provided a groundwater transit flow rate estimate of 57.5 ml/min passing through the piezometer screen. (b) The measured groundwater flux is 0.73 m/d. (C_w* = normalized Uranine tracer concentration C_w / C_{inj})

Fig. 8: Experimental results in piezometer Pz9 (see Figures 2 and 3 for location). The dilution experiment provided a groundwater flux estimate of 0.84 m/d. (C_w* = normalized Uranine tracer concentration C_w / C_{inj})

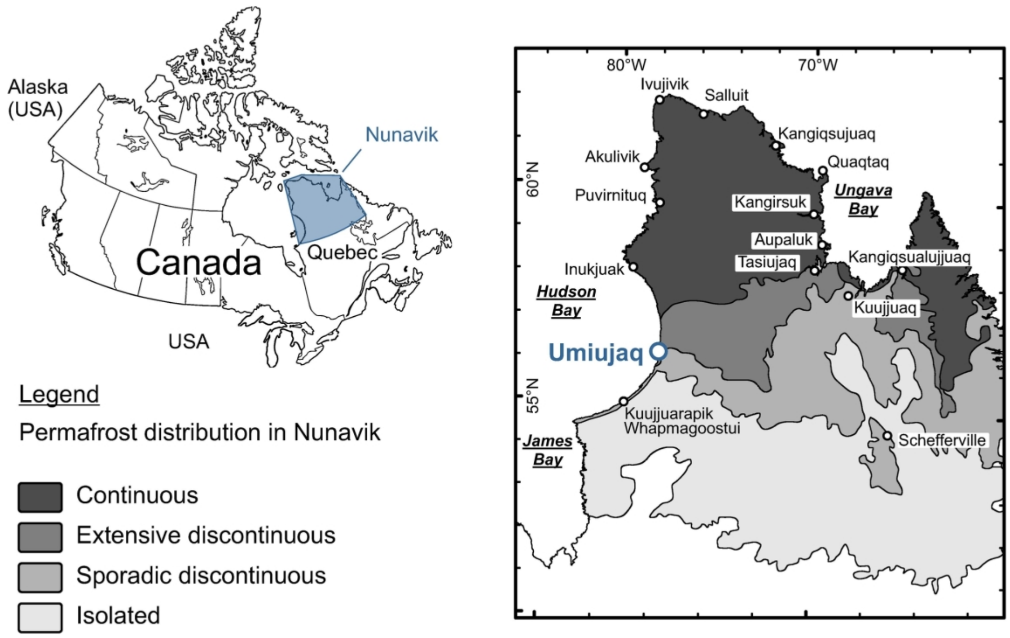

Fig. 1: Maps of Canada and permafrost extent and types in Nunavik (Quebec; Allard and Lemay 2012). The experiments were carried out near Umiujaq, an Inuit community located on the east coast of Hudson Bay, in the discontinuous permafrost zone, in Nunavik (Quebec), Canada. The studied 2 km² watershed is located near Umiujaq at the northern end of Lake Tasiujaq, into which it drains.

174x109mm (300 x 300 DPI)

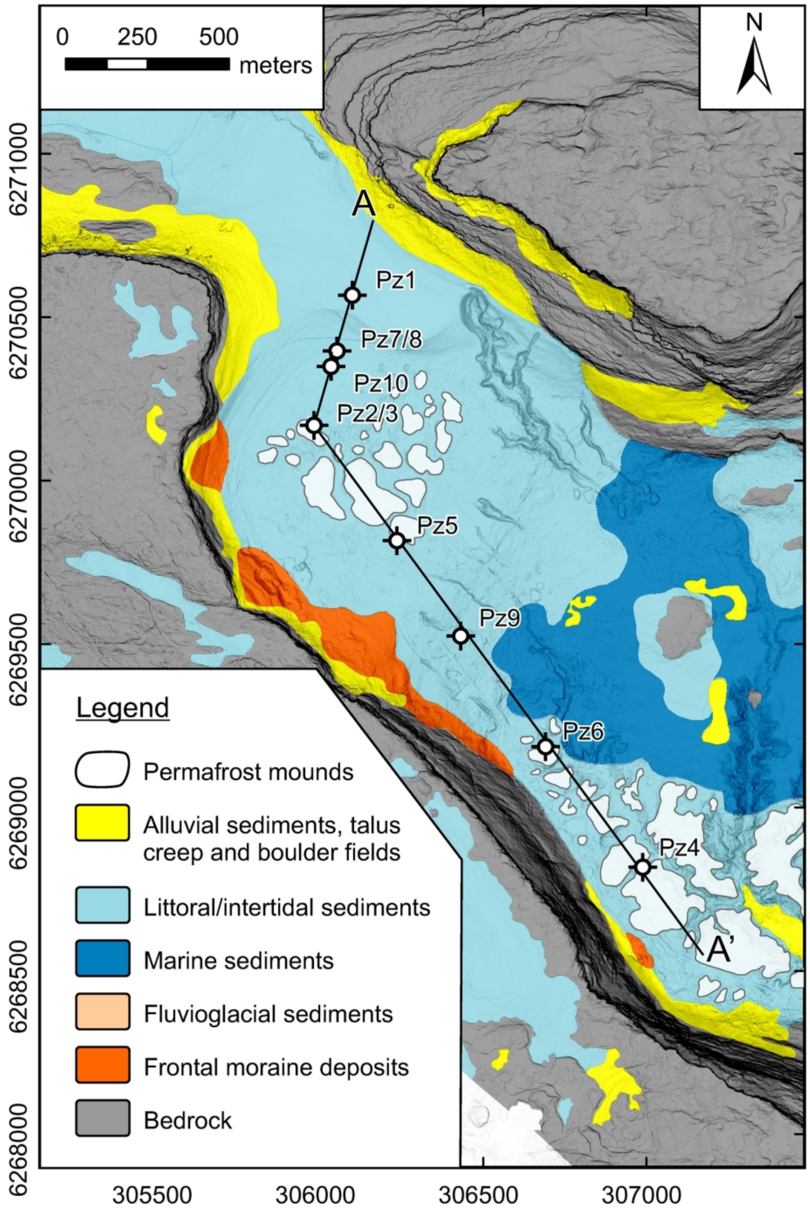

Fig. 2: Map of the Quaternary deposits in the Tasiapik Valley. Location of the piezometers and cross-section in the Tasiapik Valley. Projected coordinate system: NAD 1983 MTM Zone 9.

140x209mm (300 x 300 DPI)

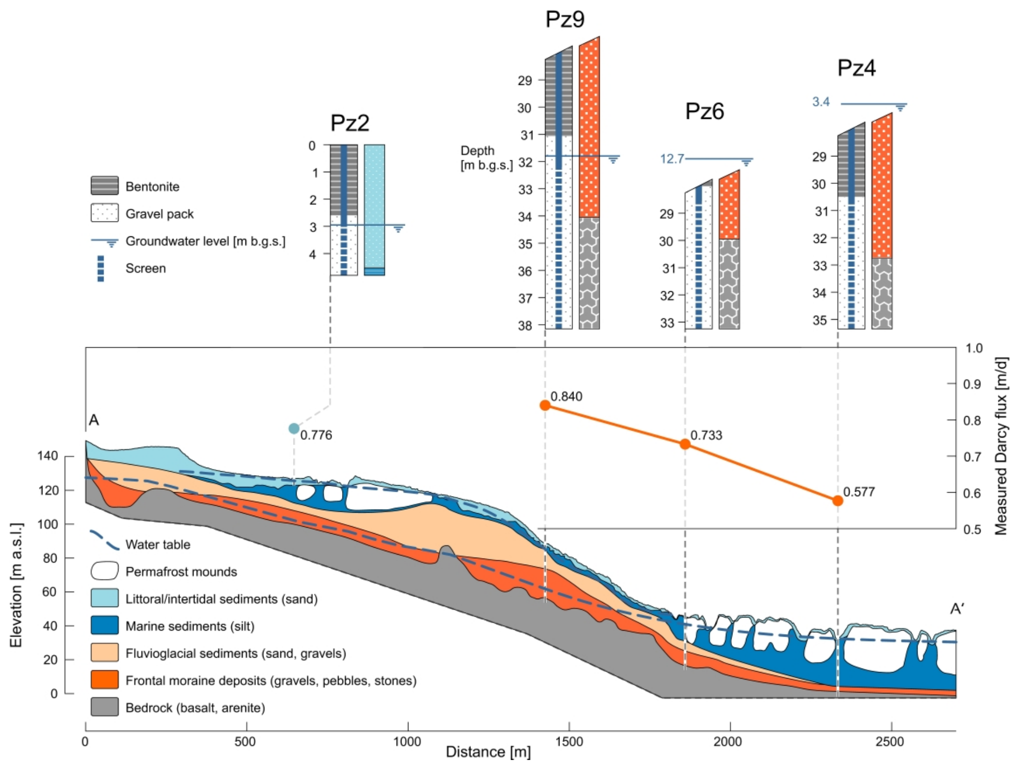

Fig. 3: Cross-section of Quaternary deposits in the Tasiapik Valley (see Figure 2 for location). The upper sediment layers are composed of littoral sands and marine silts invaded by permafrost. The uppermost sand layer contains an unconfined perched aquifer. A deep aquifer is found in the coarse-grained fluvioglacial sediments at depth overlying the bedrock. Among the four tested piezometers, three are located in the deep aquifer while one is in the surficial aquifer. Note: for piezometers Pz4, Pz6, and Pz9, only the part of each screen that is located in the deep aquifer is considered representative of the flow system for the calculation of groundwater fluxes. The Darcy fluxes measured within the piezometers installed in the fluvioglacial sediments decrease along the flow direction of the Tasiapik Valley toward Lake Tasiujaq.

551x413mm (600 x 600 DPI)

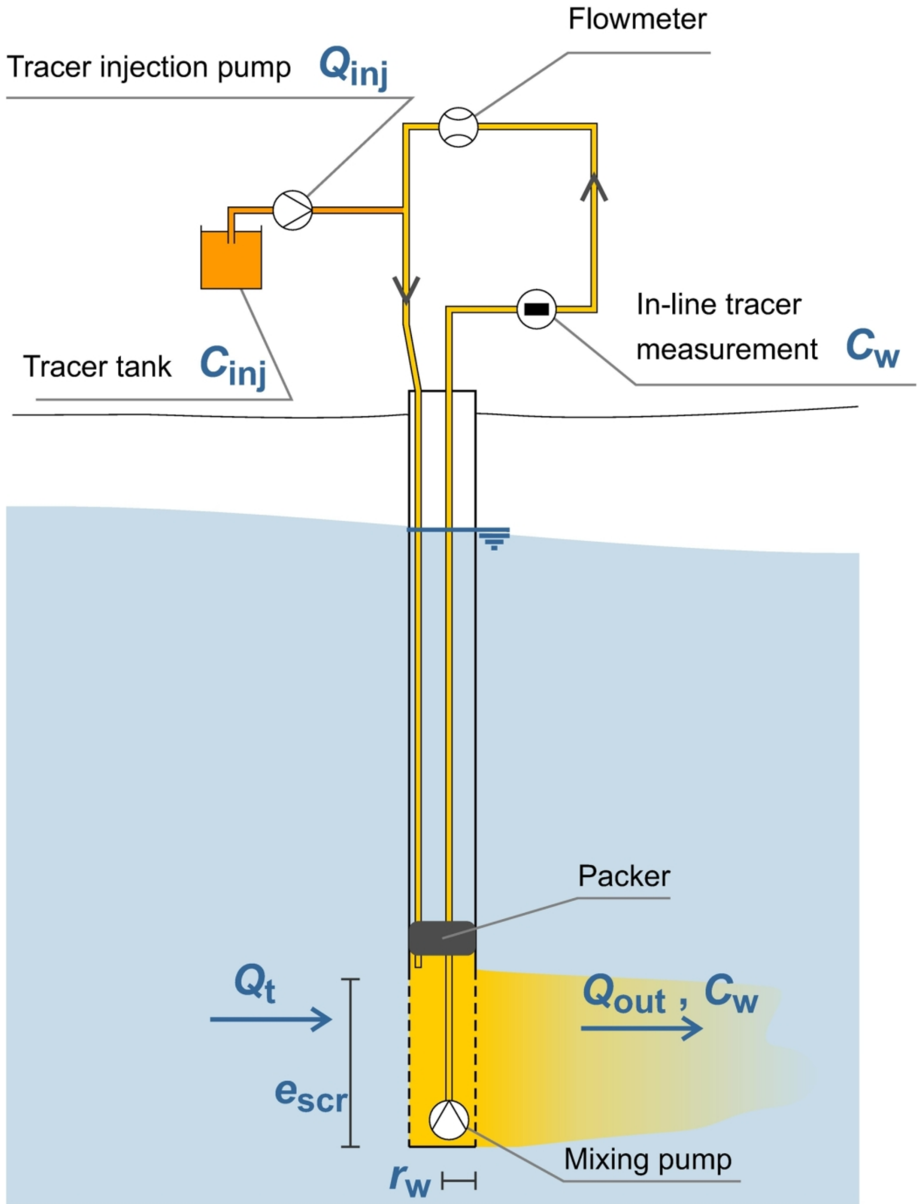

Fig. 4: Experimental setup of the FVPDM. The water volume within the well is constantly mixed using a pump and circulated to the surface, where a tracer is injected using a dosing pump. Tracer concentration in the loop is monitored using a field fluorometer placed in-line. A packer was installed in piezometers Pz4 and Pz6 to limit the mixing volume, hence shortening the time required for the FVPDM experiment.

151x198mm (300 x 300 DPI)

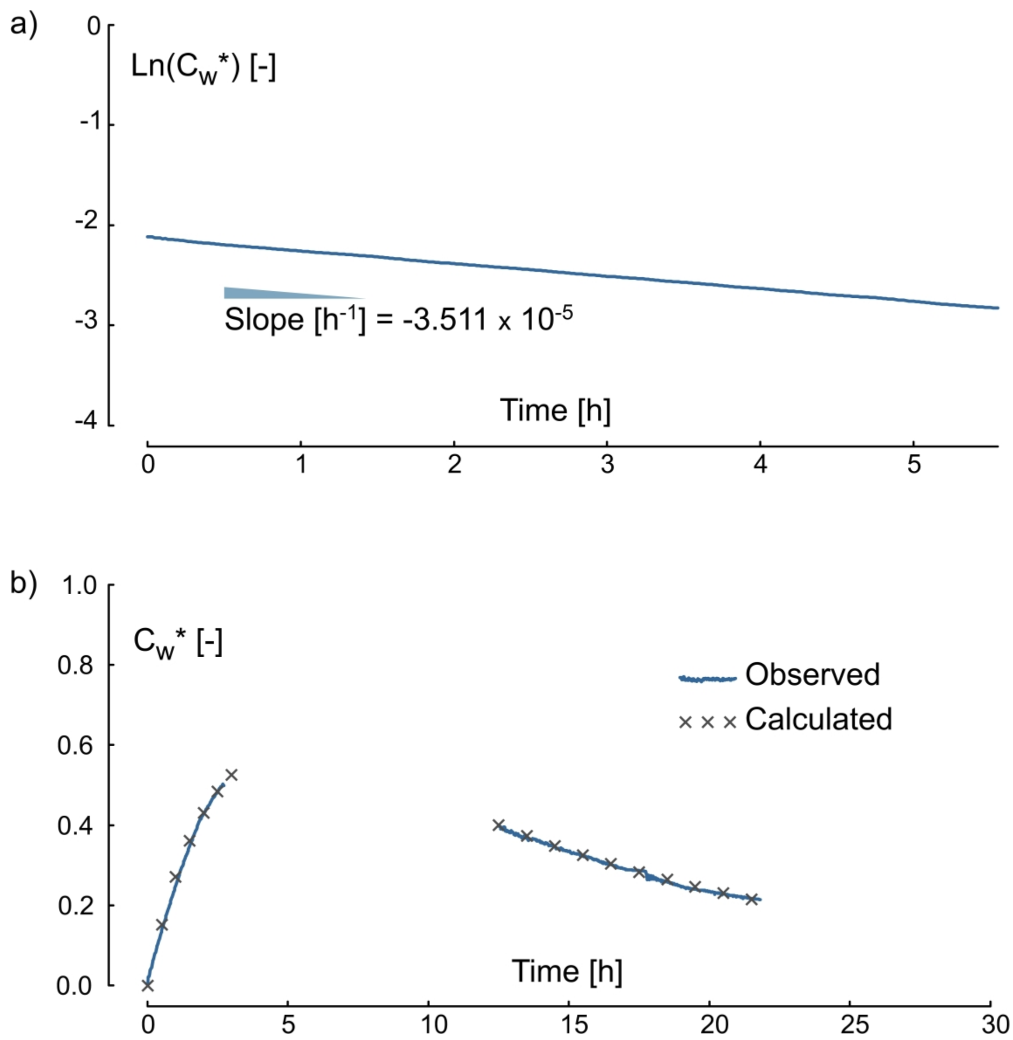

Fig. 5: Experimental results in piezometer Pz2 (see Figures 2 and 3 for location). (a) The first PDM dilution experiment provided a groundwater transit flow rate estimate of 15.2 ml/min passing through the piezometer screen. (b) The estimated groundwater flux is 0.78 m/d. A failure of the mixing pump prevented the measurement and stabilization of the tracer concentration during the FVPDM experiment. (Cw* = normalized Uranine tracer concentration Cw / Cinj)

673x690mm (600 x 600 DPI)

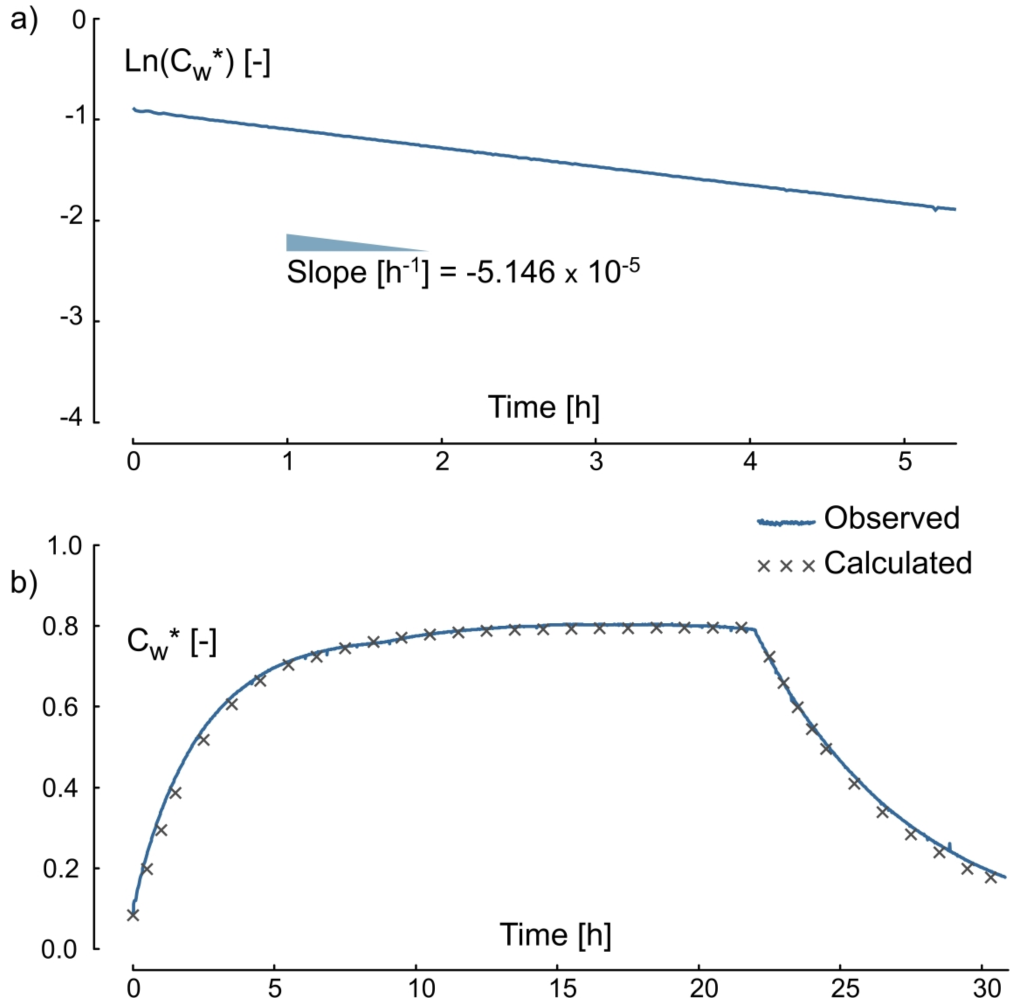

Fig. 6: Experimental results in piezometer Pz4 (see Figures 2 and 3 for location). (a) The first dilution experiment provided a groundwater transit flow rate estimate of 36.7 ml/min passing through the piezometer screen. (b) The measured groundwater flux is 0.58 m/d. (Cw* = normalized Uranine tracer concentration Cw / Cinj)

669x663mm (600 x 600 DPI)

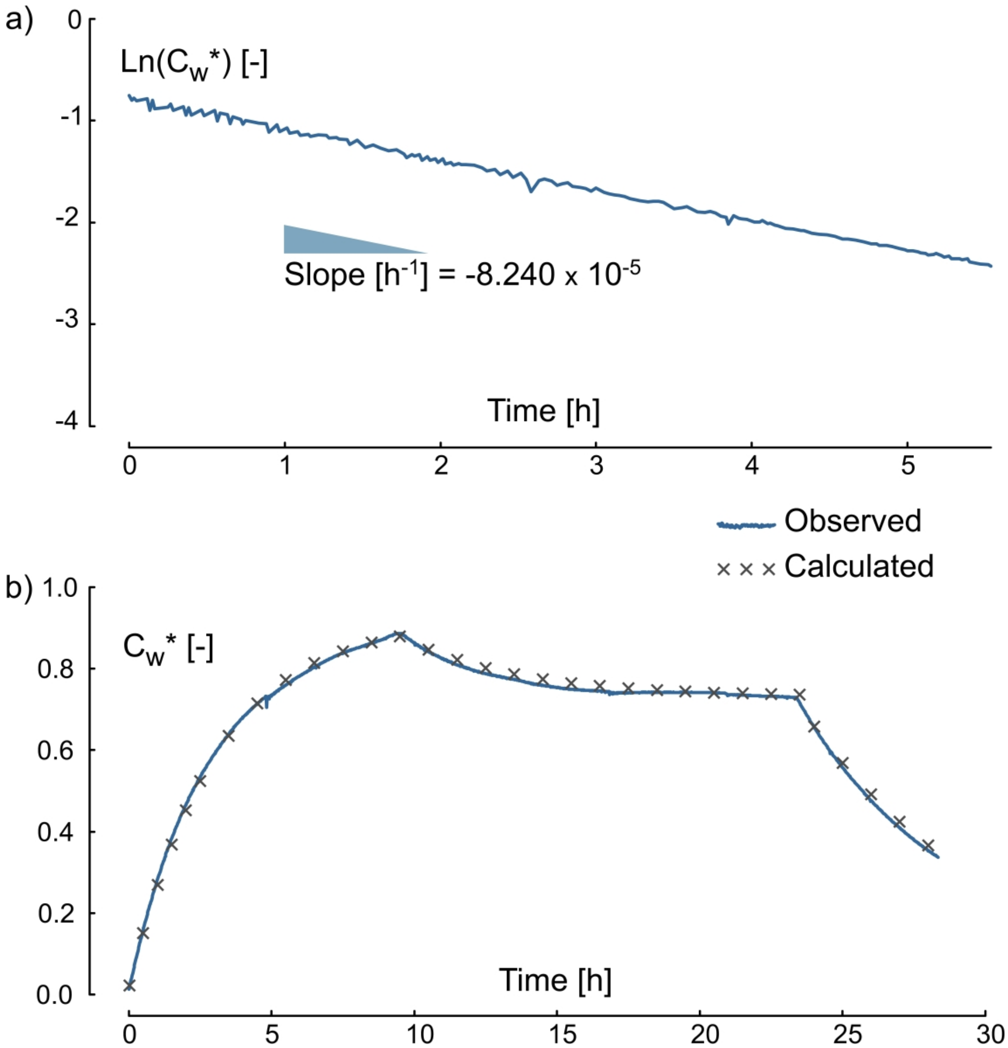

Fig. 7: Experimental results in piezometer Pz6 (see Figures 2 and 3 for location). (a) The first dilution experiment provided a groundwater transit flow rate estimate of 57.5 ml/min passing through the piezometer screen. (b) The measured groundwater flux is 0.73 m/d. (Cw* = normalized Uranine tracer concentration Cw / Cinj)

663x688mm (600 x 600 DPI)

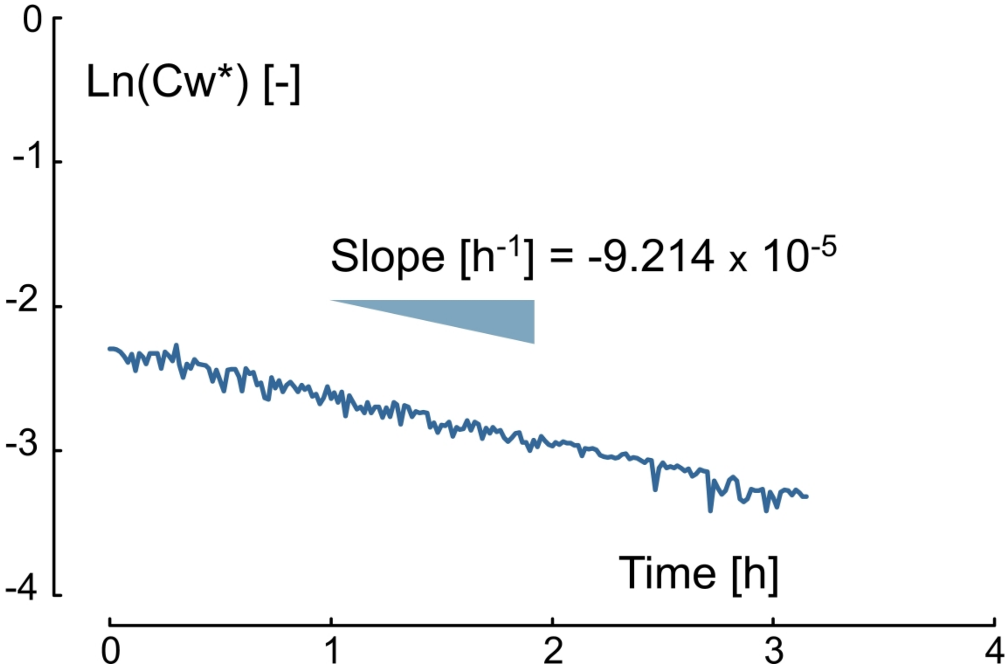

Fig. 8: Experimental results in piezometer Pz9 (see Figures 2 and 3 for location). The dilution experiment provided a groundwater flux estimate of 0.84 m/d. (Cw* = normalized Uranine tracer concentration Cw / Cinj)

466x308mm (300 x 300 DPI)